
REPORT No. 275

**THE EFFECT OF THE WALLS IN CLOSED TYPE
WIND TUNNELS**

By **GEORGE J. HIGGINS**
Langley Memorial Aeronautical Laboratory



REPORT No. 275

THE EFFECT OF THE WALLS IN CLOSED TYPE WIND TUNNELS

By GEORGE J. HIGGINS

SUMMARY

A series of tests has been conducted during the period 1925-1927 by the National Advisory Committee for Aeronautics in the variable-density wind tunnel on several airfoil models of different sizes and sections to determine the effect of tunnel-wall interference and to determine a correction which can be applied to reduce the error caused thereby. The use of several empirical corrections was attempted with little success. The Prandtl theoretical corrections give the best results, and their use is recommended for correcting closed wind tunnel results to the conditions of free air.

An appendix is attached wherein the experimentally determined effect of the walls on the tunnel velocity very close to their surface is given. This is of special interest because a "scale effect" was found in the boundary layer with a change in the density of the tunnel air.

INTRODUCTION

When tests are made on models in wind tunnels to determine their aerodynamic characteristics, the results obtained are not truly representative because of the limited air jet of the tunnel. The boundary of the jet, whether free or inclosed by walls, affects the flow to a considerable extent. This effect has been considered theoretically and a method devised for correcting the results from wind-tunnel tests.

Experimental confirmation of this correction is extremely desirable, and though such confirmation has been obtained in wind tunnels in Europe, tests for that purpose had not been made in wind tunnels of the National Advisory Committee for Aeronautics. A series of tests was therefore authorized for the variable-density wind tunnel.

This investigation consisted of force tests on several airfoil models of the N. A. C. A.-M6 section having a constant chord and a varying span. From these tests some idea of the effect of the tunnel walls can be ascertained.

Data from previous tests on models of the M6 airfoil section of different sizes, aspect ratio 6, were available and were used in the analysis. For further confirmation, and in conjunction with another investigation, tests were made on three airfoil models of the R. A. F. 19 section, each having the same aspect ratio but different areas.

TESTS

The tests on the N. A. C. A.-M6 airfoils in this investigation were conducted after the usual method employed for force tests in the variable-density wind tunnel, as described in reference 1. The angle of attack was varied from -3° to $+21^\circ$; runs were made at three densities or Reynolds Numbers, corresponding to tank pressures of about 1, 15, and 20 atmospheres. The R. A. F. 19 series was similarly tested, but at different values of the Reynolds Number.

The N. A. C. A.-M6 section model was $4\frac{1}{2}$ inches by 36 inches in plan. It was tested in this form, of aspect ratio 8, and then cut off on the ends so that the span became 32 inches, giving the model an aspect ratio of 7.12. This procedure was repeated, making tests on the model with aspect ratios of 6, 5.33, and 4.44. The R. A. F. 19 models were all of aspect ratio 6 with plan form dimensions of 4 inches by 24 inches, 5 inches by 30 inches, and 6 inches by 36 inches. All models were made of duralumin and machined to within ± 0.002 inch of the specified ordinates.

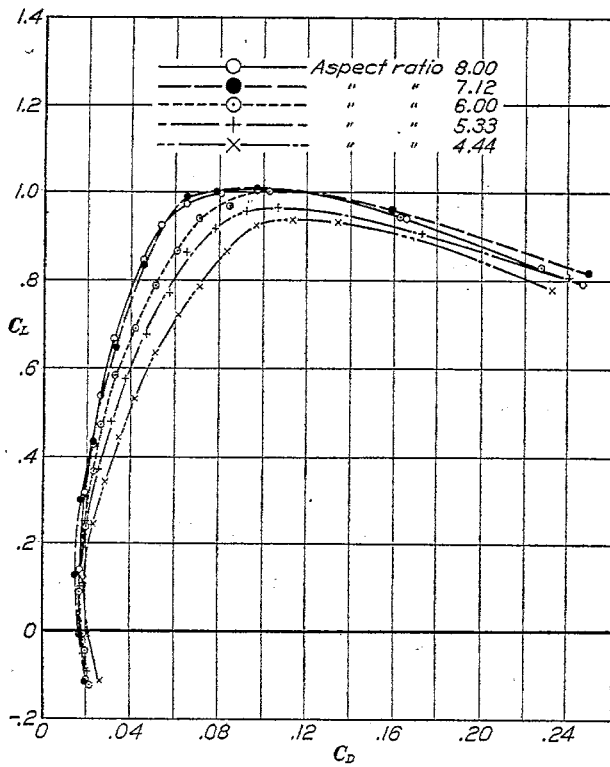


FIG. 1.—N. A. C. A. -M6 airfoil of various aspect ratios, as observed in tunnel, 1 atmosphere

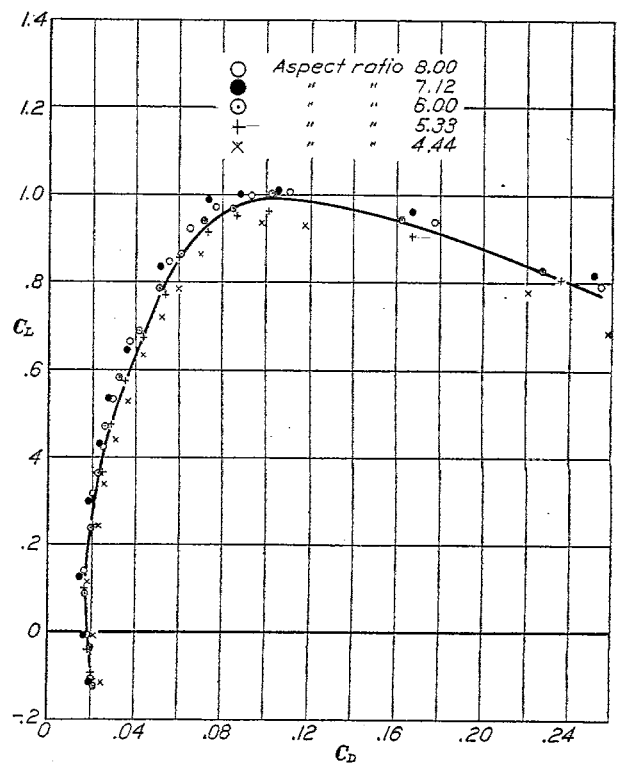


FIG. 2.—N. A. C. A. -M6 airfoil of various aspect ratios, corrected to aspect ratio 6.00; no correction for tunnel wall; 1 atmosphere

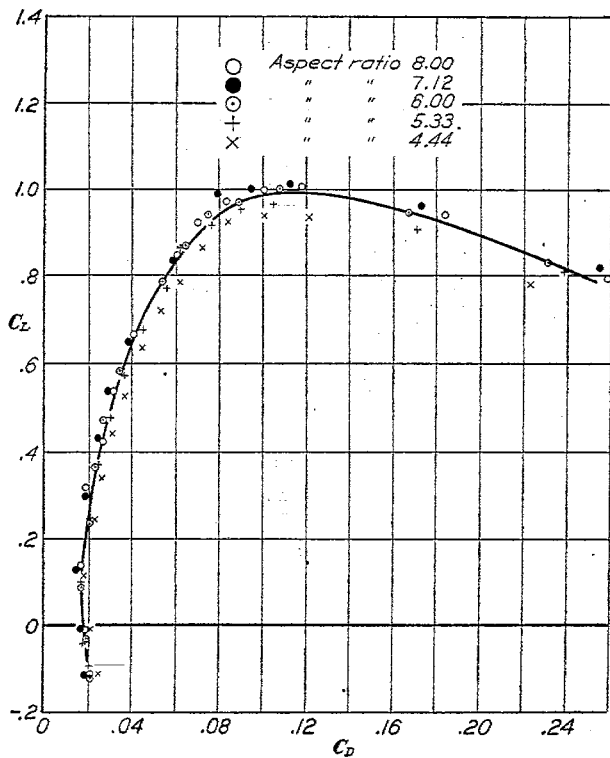


FIG. 3.—N. A. C. A. -M6 airfoil of various aspect ratios, corrected to aspect ratio 6.00 in free air, 1 atmosphere

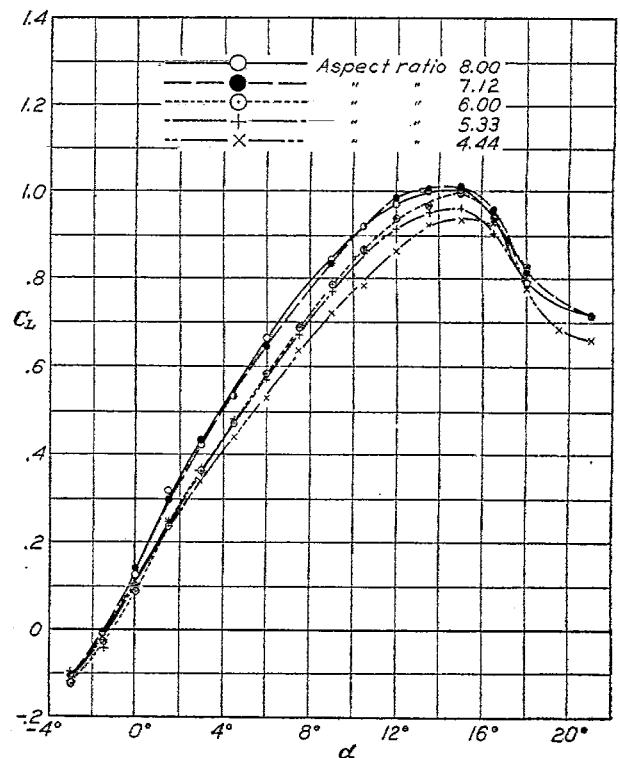


FIG. 4.—N. A. C. A. -M6 airfoil of various aspect ratios, as observed in tunnel, 1 atmosphere

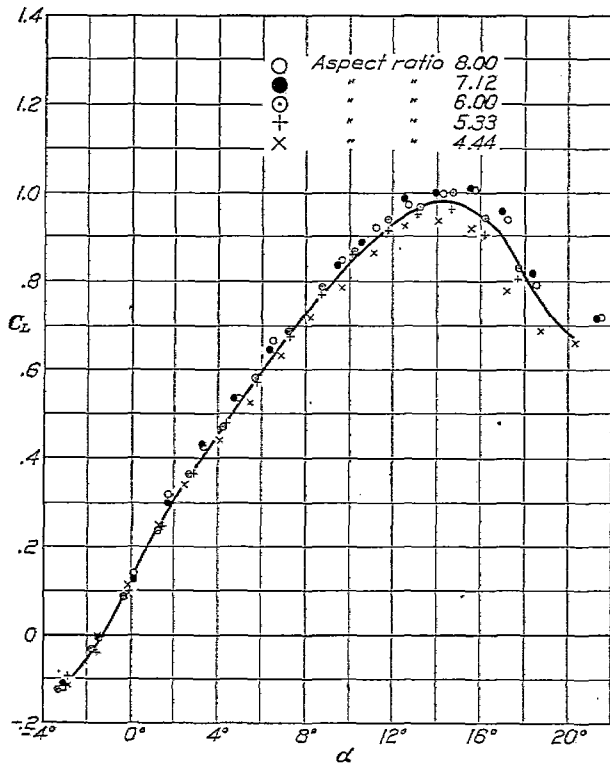


FIG. 5.—N. A. C. A.—M6 airfoil of various aspect ratios, corrected to aspect ratio 6.00; no correction for tunnel wall; 1 atmosphere

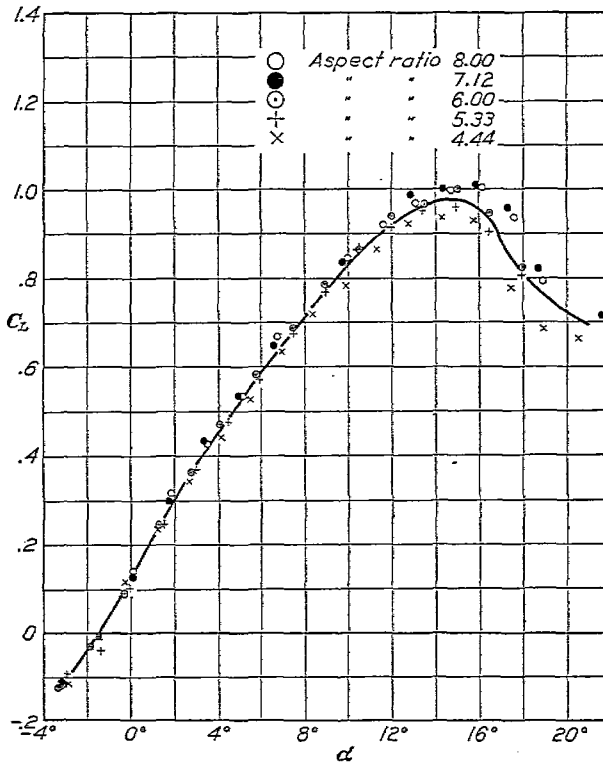


FIG. 6.—N. A. C. A.—M6 airfoil of various aspect ratios, corrected to aspect ratio 6.00 in free air, 1 atmosphere

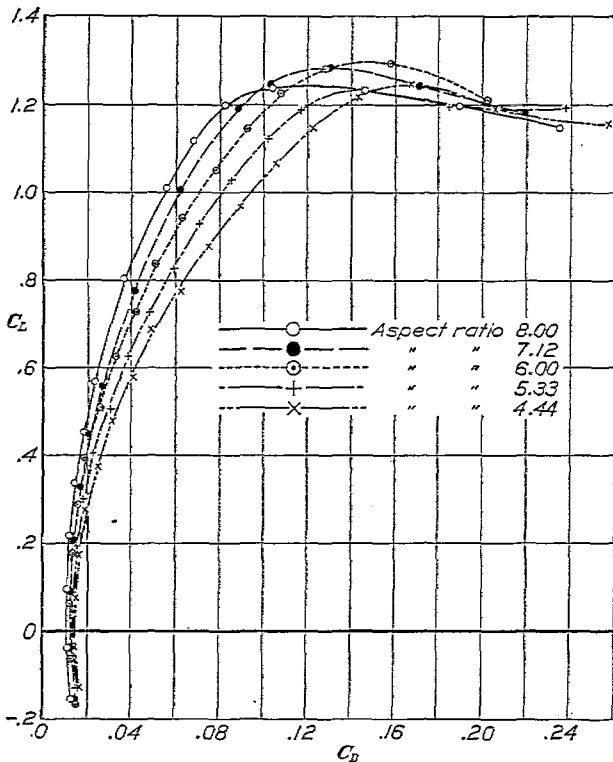


FIG. 7.—N. A. C. A.—M6 airfoil of various aspect ratios, as observed in tunnel, 15 atmospheres

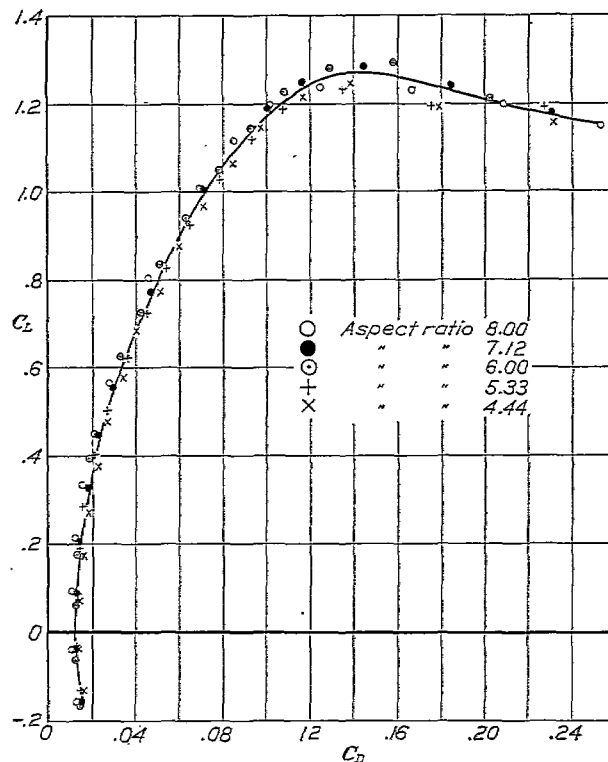


FIG. 8.—N. A. C. A.—M6 airfoil of various aspect ratios, corrected to aspect ratio 6.00; no correction for tunnel wall; 15 atmospheres

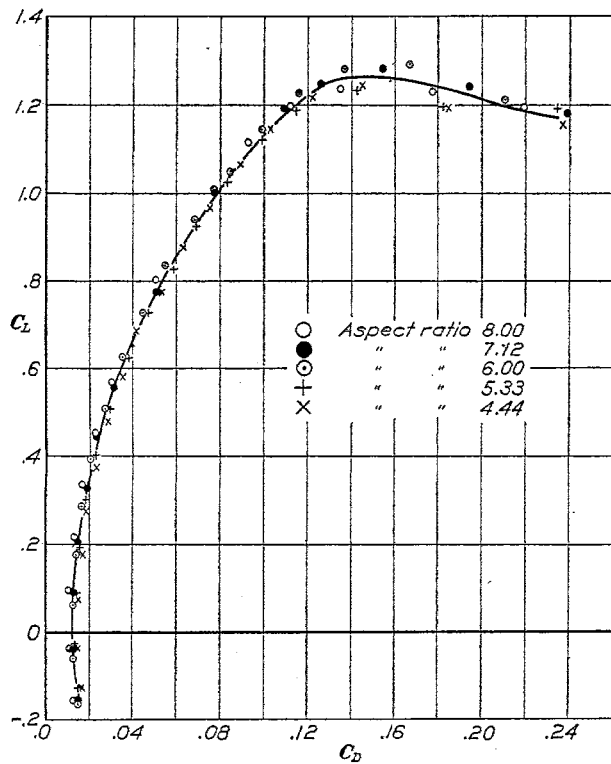


FIG. 9.—N. A. C. A.-M6 airfoil of various aspect ratios, corrected to aspect ratio 6.00 in free air, 15 atmospheres

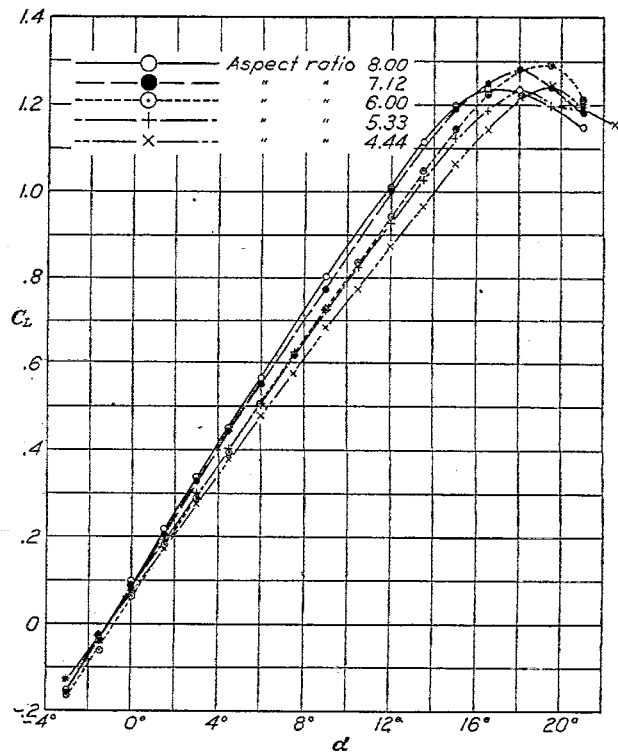


FIG. 10.—N. A. C. A.-M6 airfoil of various aspect ratios, as observed in tunnel, 15 atmospheres

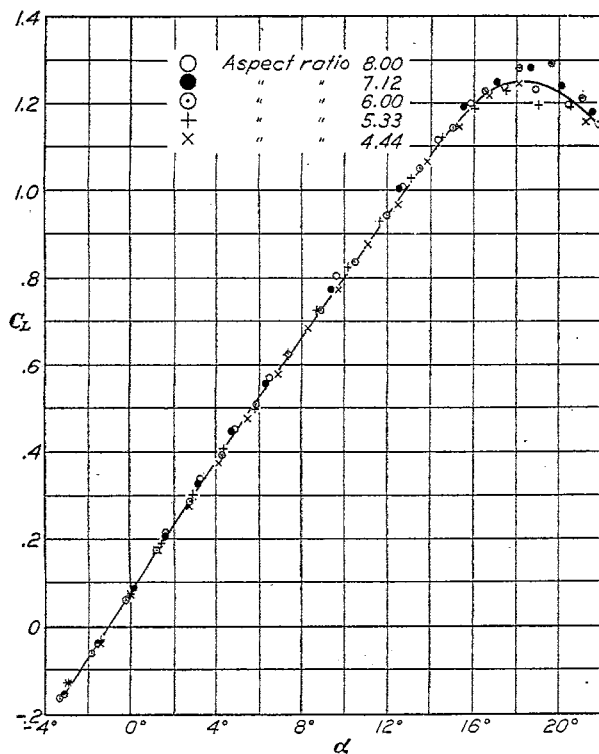


FIG. 11.—N. A. C. A.-M6 airfoil of various aspect ratios, corrected to aspect ratio 6.00; no correction for tunnel wall; 15 atmospheres

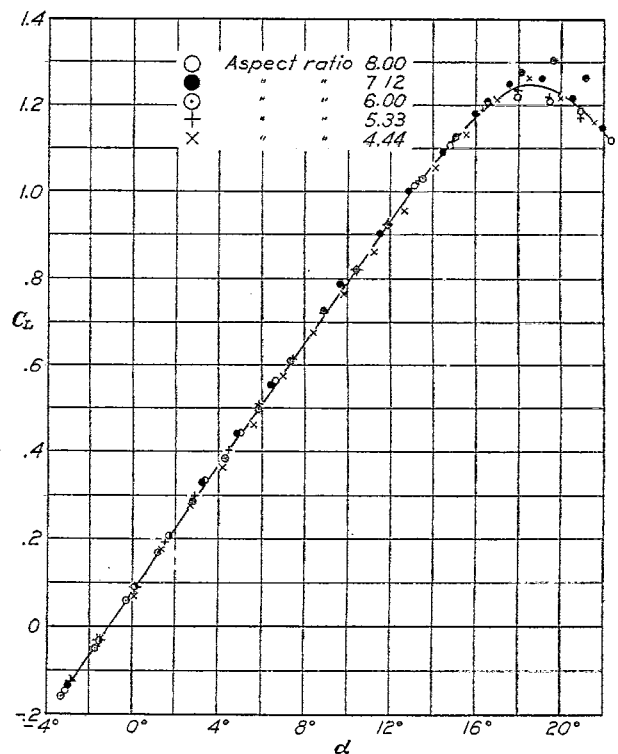


FIG. 12.—N. A. C. A.-M6 airfoil of various aspect ratios, corrected to aspect ratio 6.00 in free air, 15 atmospheres

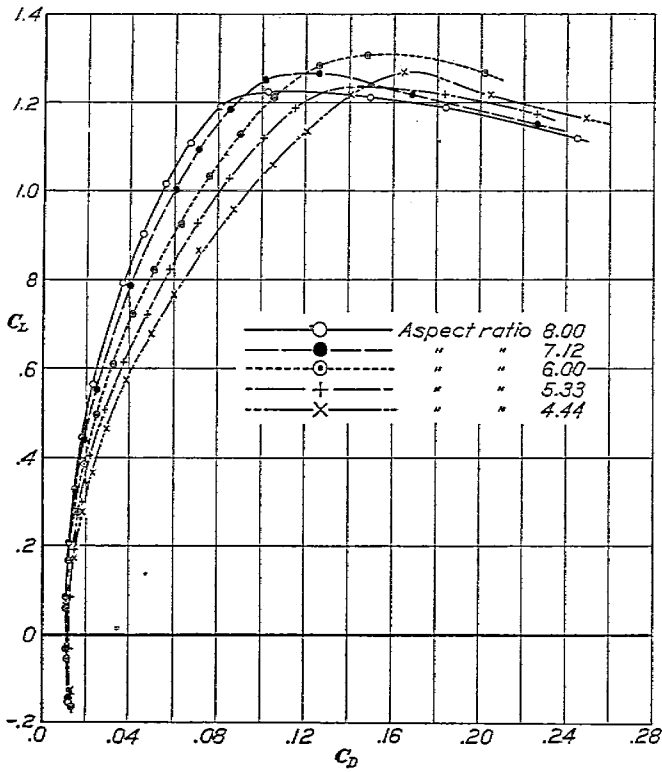


FIG. 13.—N. A. C. A.-M6 airfoil of various aspect ratios, as observed in tunnel, 20 atmospheres

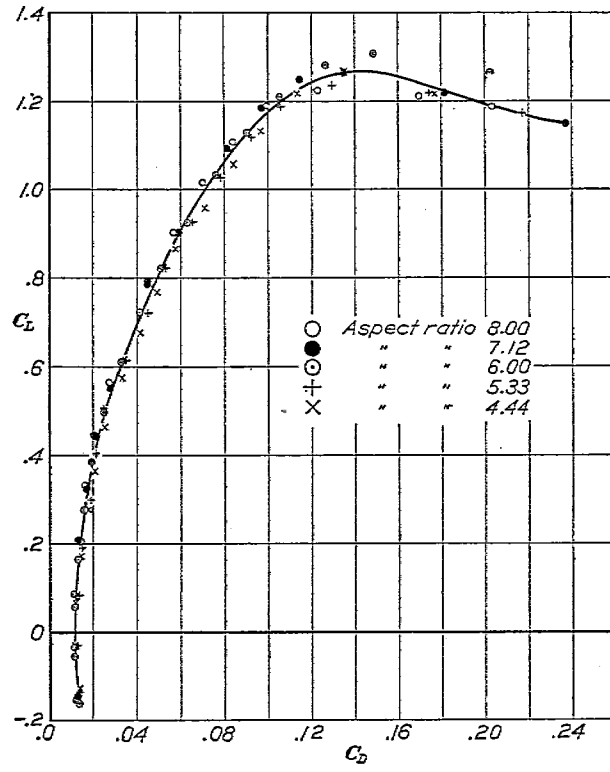


FIG. 14.—N. A. C. A.-M6 airfoil of various aspect ratios, corrected to aspect ratio 6.00; no correction for tunnel walls; 20 atmospheres

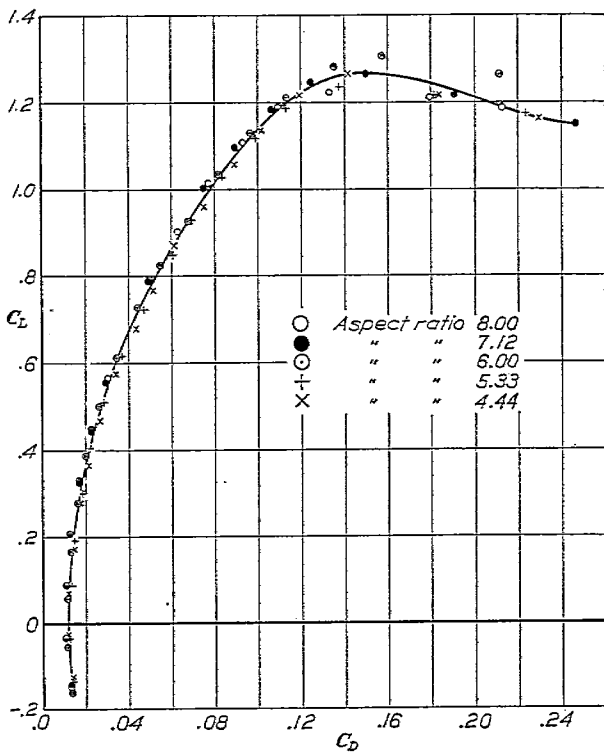


FIG. 15.—N. A. C. A.-M6 airfoil of various aspect ratios, corrected to aspect ratio 6.00 in free air, 20 atmospheres

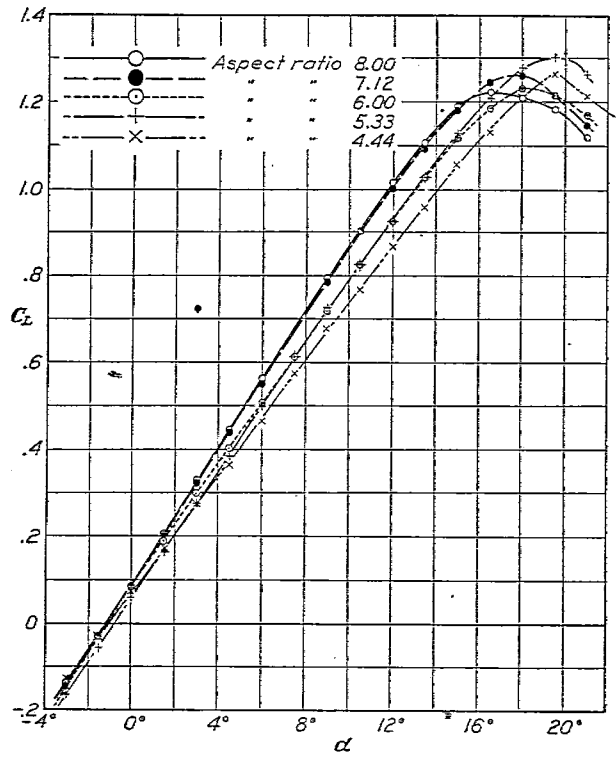


FIG. 16.—N. A. C. A.-M6 airfoil of various aspect ratios, as observed in tunnel, 20 atmospheres

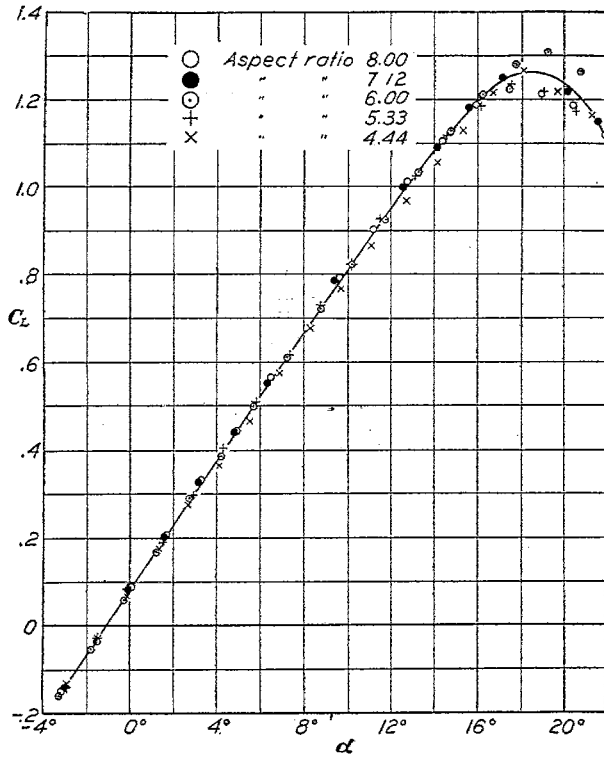


FIG. 17.—N. A. C. A.-M6 airfoil of various aspect ratios, corrected to aspect ratio 6.00; no correction for tunnel walls; 20 atmospheres

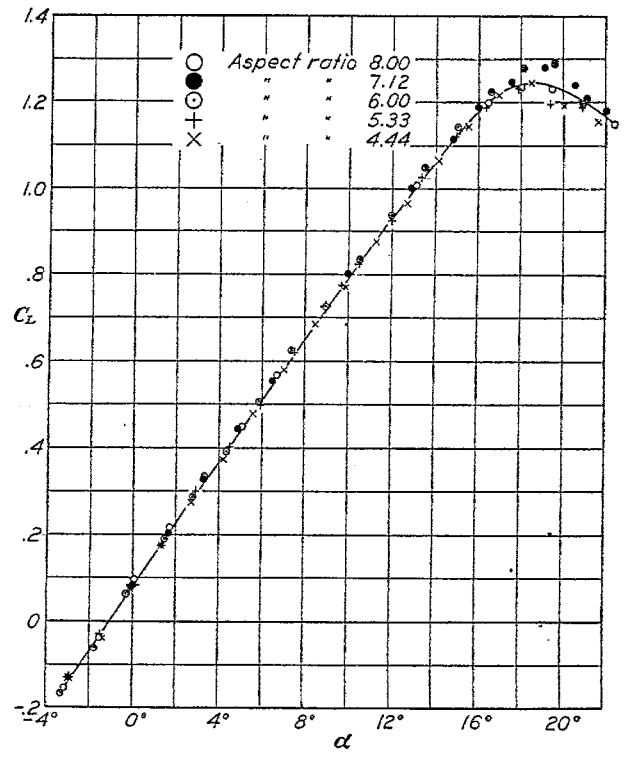


FIG. 18.—N. A. C. A.-M6 airfoil of various aspect ratios, corrected to aspect ratio 6.00 in free air, 20 atmospheres

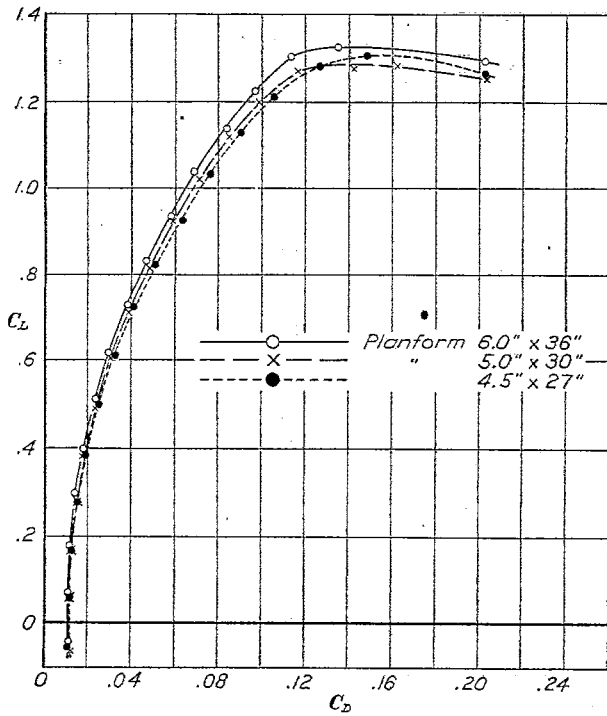


FIG. 19.—As observed in tunnel

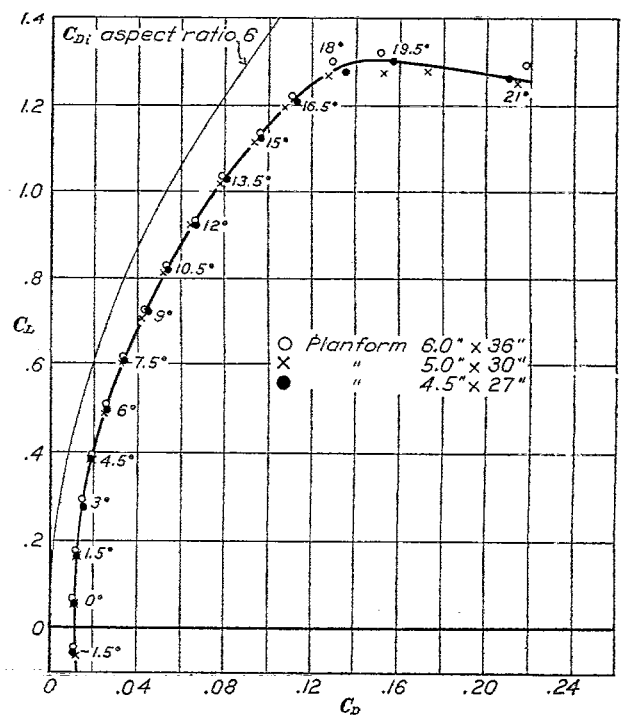


FIG. 20.—Corrected for wall interference

N. A. C. A.-M6 airfoils of various sizes; aspect ratio 6.00; 20 atmospheres

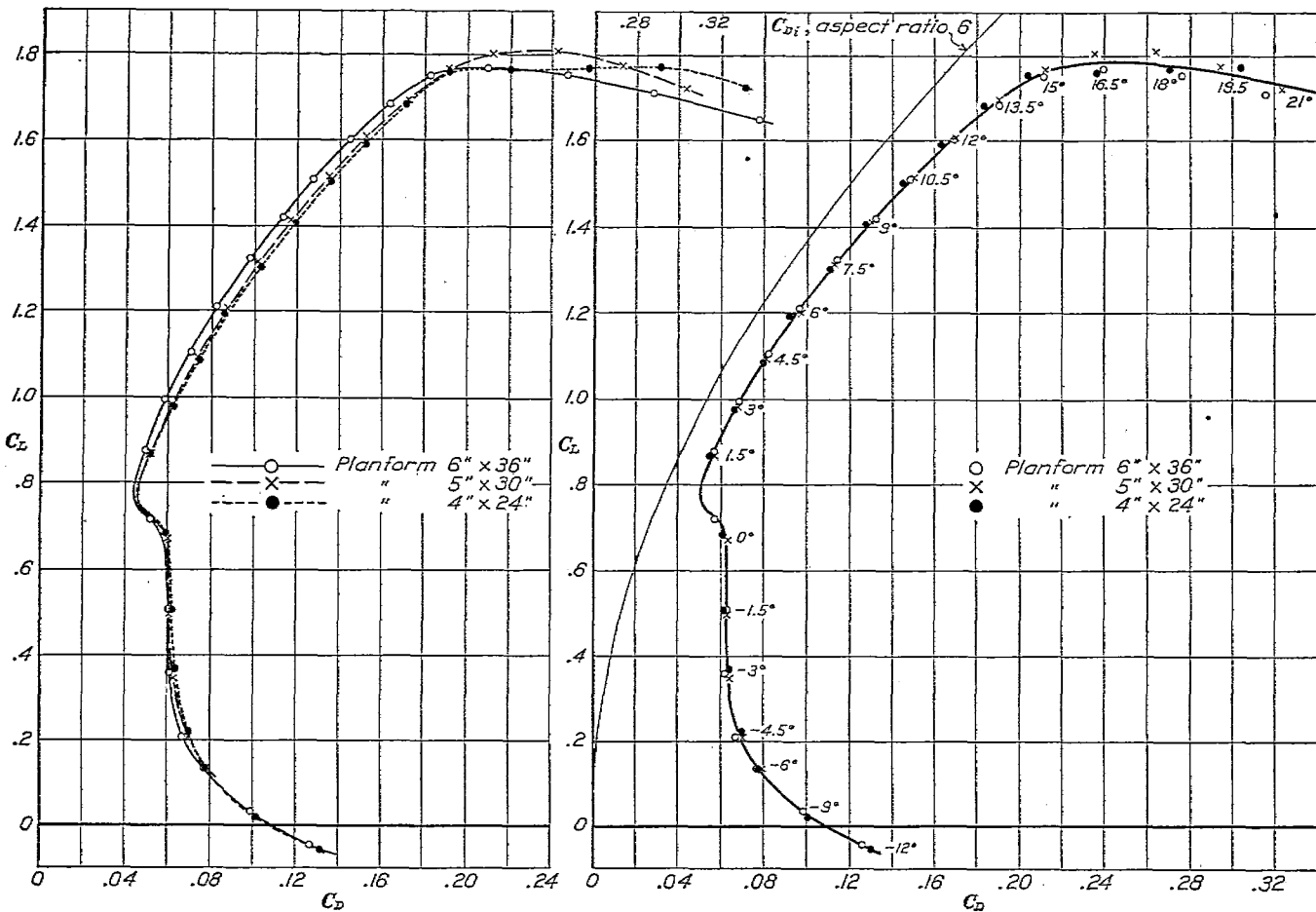


FIG. 21.—As observed in tunnel

FIG. 22.—Corrected for wall interference

R. A. F. airfoils of various sizes; aspect ratio 6.00; average Reynolds Number 530,000

RESULTS AND DISCUSSION

Readings of lift and drag at various angles of attack were obtained and reduced to absolute coefficients. Those obtained from the tests on models of aspect ratios other than 6 were reduced to coefficients for that aspect ratio as noted in the figures, using the Prandtl induced drag equation. These data were then plotted in various forms to determine the existence of any effects that might possibly be attributed to the interference of the walls. Numerous empirical corrections and the Prandtl theoretical corrections (references 2 and 3) were applied to find whether better agreement between the results from the different models could be obtained.

None of the empirical corrections tried was very satisfactory, while the theoretical corrections of Prandtl gave results which were in good agreement. These corrections are:

$$\Delta C_{D_i} = \frac{C_L^2 S}{2\pi D^2}$$

and

$$\Delta \alpha_i = \frac{C_L S}{2\pi D^2}$$

to be added to C_D and α , respectively,

where

- C_L = lift coefficient.
- C_{D_i} = induced drag coefficient.
- α_i = induced angle.
- S = area of the airfoil.
- D = diameter of the tunnel.

A comparison of the results may be had by referring to the figures which are listed below:
 FIGURE 1.—N. A. C. A.—M6 airfoil of various aspect ratios— C_L vs. C_D —1 atm., as observed in tunnel.

FIGURE 2.—N. A. C. A.—M6 airfoil of various aspect ratios— C_L vs. C_D —1 atm., corrected to aspect ratio 6 (assuming no wall correction necessary).

FIGURE 3.—N. A. C. A.—M6 airfoil of various aspect ratios— C_L vs. C_D —1 atm., corrected to aspect ratio 6 with the Prandtl wall interference correction.

FIGURE 4. }
 FIGURE 5. } Same as above, C_L vs. α —1 atm.
 FIGURE 6. }

FIGURE 7. }
 FIGURE 8. } Same as above, C_L vs. C_D —15 atm.
 FIGURE 9. }

FIGURE 10. }
 FIGURE 11. } Same as above, C_L vs. α —15 atm.
 FIGURE 12. }

FIGURE 13. }
 FIGURE 14. } Same as above, C_L vs. C_D —20 atm.
 FIGURE 15. }

FIGURE 16. }
 FIGURE 17. } Same as above, C_L vs. α —20 atm.
 FIGURE 18. }

FIGURE 19.—N. A. C. A.—M6 airfoils of three sizes, A. R. 6, C_L vs. C_D —20 atm., as observed in tunnel.

FIGURE 20.—Same as above, C_L vs. C_D , corrected for wall interference.

FIGURE 21.—R. A. F. 19 airfoils of three sizes, A. R. 6, C_L vs. C_L , R. N. 530,000, as observed in the tunnel.

FIGURE 22.—Same as above, C_L vs. C_D , corrected for wall interference.

It may be seen from an inspection of the above figures that in every case there is better agreement between the results from the different models after the Prandtl corrections have been applied. The improved agreement is found not only for the drag coefficient but also for the angle of attack. The corrections are valid for any airfoil section and for any plan form.

CONCLUSION

Test data from closed wind tunnels on airfoil models of a given section, but having various plan forms, show better agreement when corrected for tunnel wall interference by the Prandtl formulas. The use of these formulas is therefore recommended for correcting wind-tunnel data to the conditions of free air.

LANGLEY MEMORIAL AERONAUTICAL LABORATORY.
 NATIONAL ADVISORY COMMITTEE FOR AERONAUTICS,
 LANGLEY FIELD, VA., May 5, 1927.

APPENDIX

PITOT TUBE SURVEY CLOSE TO WALL

INTRODUCTION

A dynamic pressure and velocity survey has been made across the throat of the variable density wind tunnel for the purpose of determining the variation, particularly near the walls of the tunnel. The results were to be used for further theoretical consideration of the "tunnel wall effect" in which the transverse velocity variation is taken into account.

METHOD OF MEASUREMENT

The survey was made by means of two bars built on the principle of a Pitot-static tube with one bar for impact pressures and one for static pressures. (See figs. 23 and 24.) Pressures were obtained at 31 points on each bar, spaced more closely near the walls, the closest point being at one-fourth inch from the wall surface. The bars were mounted in the tunnel as shown in Figure 25; and the survey was made on three different diameters. Readings were taken simultaneously at the 31 points by means of a large photomanometer.

It developed later that readings closer to the wall were necessary. For this purpose a minute Pitot tube was constructed from 0.051 inch outside diameter hypodermic tubing. Differential pressures were read between this Pitot tube and a static plate flush with the wall, 2 inches to one side and in the same transverse plane, as shown in Figure 26. Observations were taken with this arrangement at several tank pressures at distances of 1, $\frac{1}{2}$, $\frac{1}{4}$, $\frac{1}{8}$, and $\frac{1}{16}$ inch from the wall. Due to mutual interference between the Pitot tube and the wall, the 0.051-inch tube was changed to one of 0.019 inch outside diameter, and further observations were taken at $\frac{1}{8}$, $\frac{1}{16}$, $\frac{1}{32}$, and $\frac{1}{64}$ inch.

RESULTS

The results from the survey using the bars were not unusual, and for this reason the data from this portion of the survey will be omitted; an average curve for three radii, shown in Figure 30, will indicate the general character of the dynamic pressure distribution. The survey using the small Pitot tube, however, will be discussed more fully, particularly because of the information obtained in regard to the conditions close to the wall.

The observations are recorded in Tables I and II. Here also are given readings for a standard Pitot-static tube at the center of the tunnel throat, which is 60 inches in diameter. The ratios of velocities at the two points v/V_c are plotted on logarithmic scales in Figure 27, a separate curve for each tank pressure, against x , the distance from the wall. Figure 28 shows curves that have been deduced from Figure 27, plotted against the tank pressure, which is proportional to the density.

The indicated points in Figures 29 and 30 show the observations p/P_c the ratio of the dynamic pressure at the point to that at the center of the tunnel throat, plotted against x and compared with empirical curves derived from the data. Figure 30 also shows an average curve of the dynamic pressure taken by means of the bars extending across the tunnel for comparison.

DISCUSSION

The walls of a tube or wind tunnel are known to have an effect on the flow adjacent. Theoretical consideration has been given to this effect, which has also been previously studied experimentally. In general, it has been found that the velocity at the center is maintained at approximately full value within the immediate neighborhood of the wall, the so-called region of the "boundary layer." Prandtl, Blasius, v. Karman (reference 4), Van der Hegge Zijnen (reference 5), and others have made a study of this boundary layer.

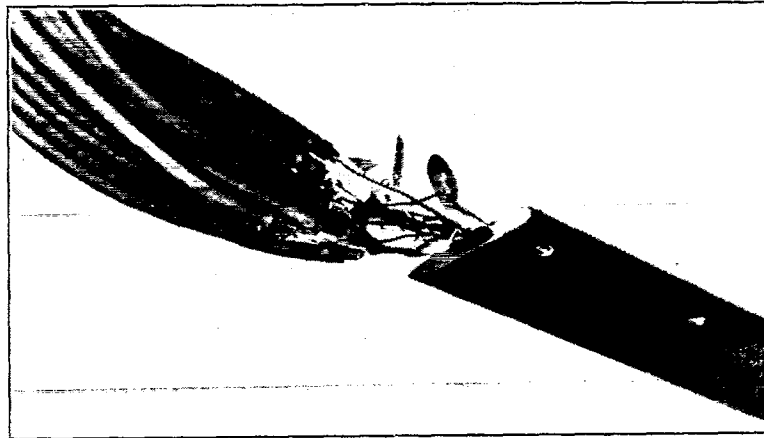


FIG. 23.—Survey bar with impact openings

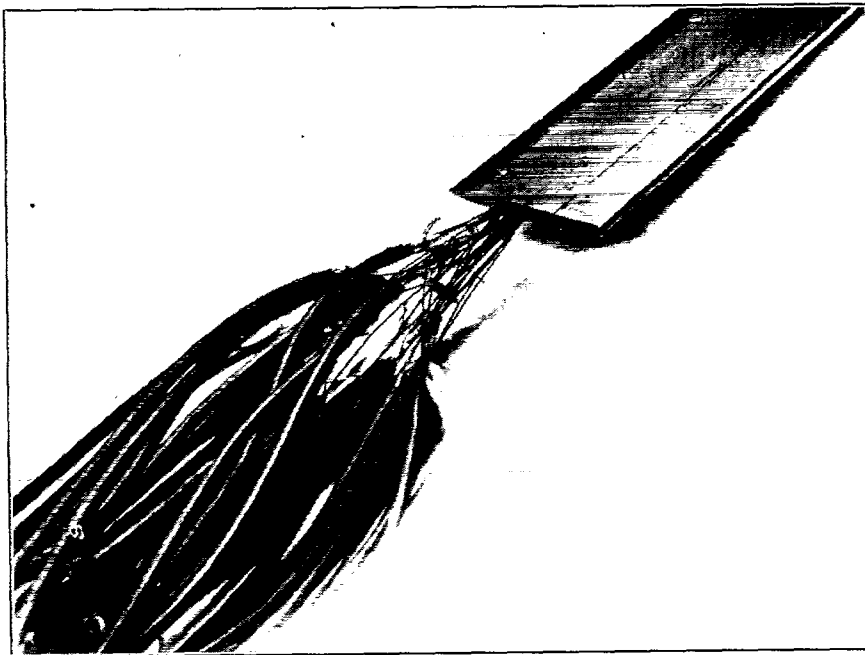


FIG. 24.—Survey bar with static openings

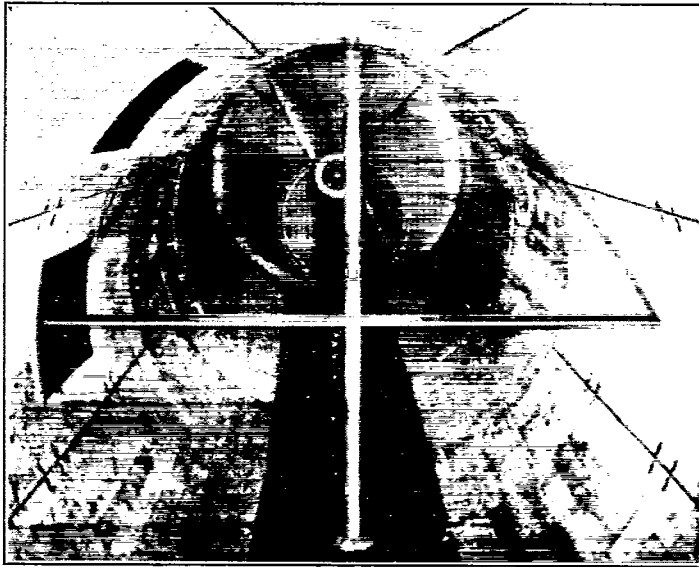


FIG. 25.—Survey bar mounted in tunnel

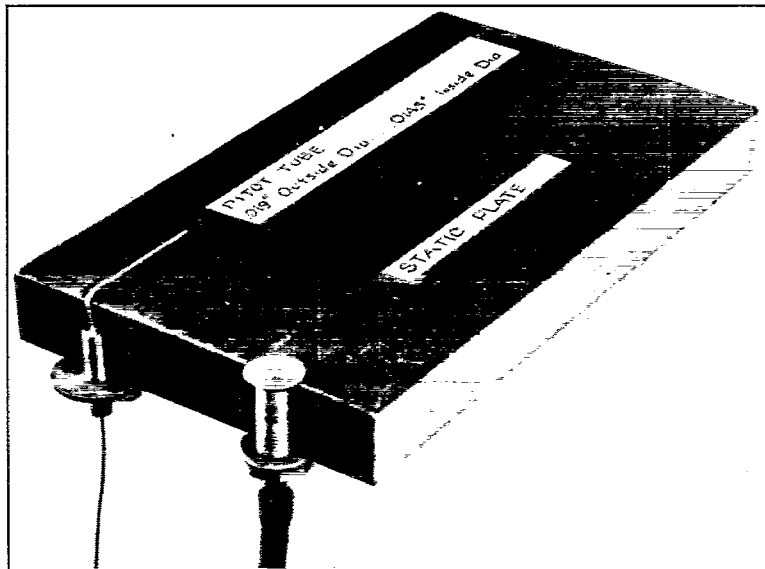


FIG. 26.—Installation of small Pitot tube and static plate

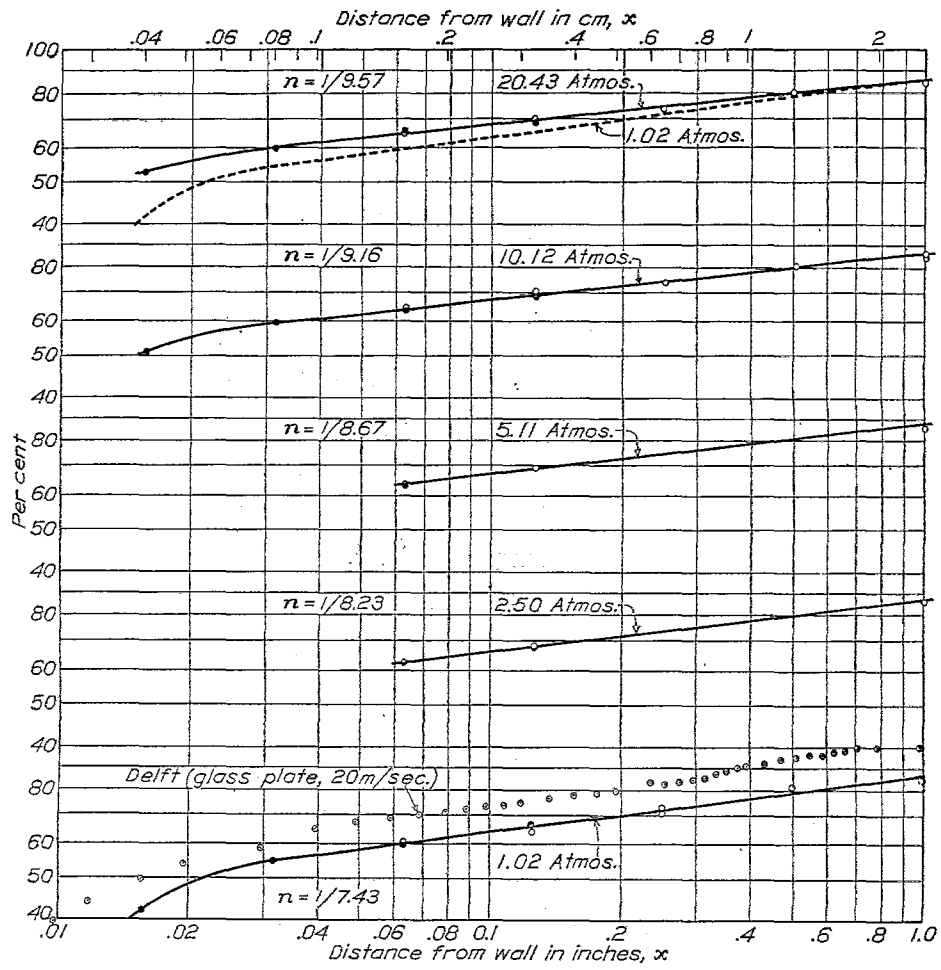


FIG. 27.—Values of η/V_e .

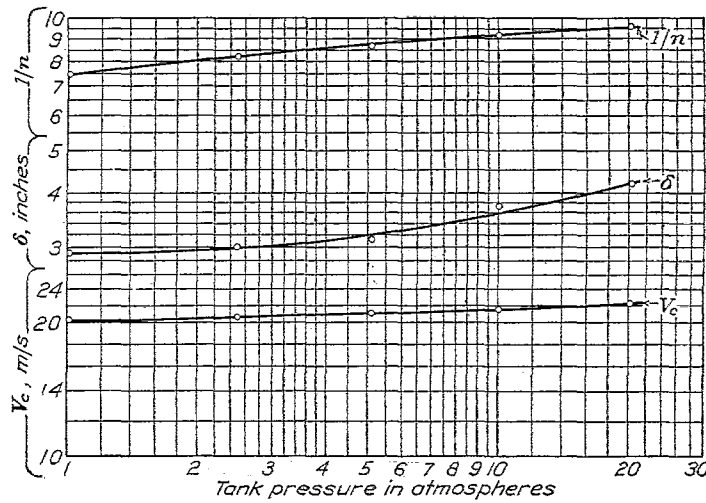


FIG. 28.—Variation of V_c, δ and $1/n$ with tank pressure

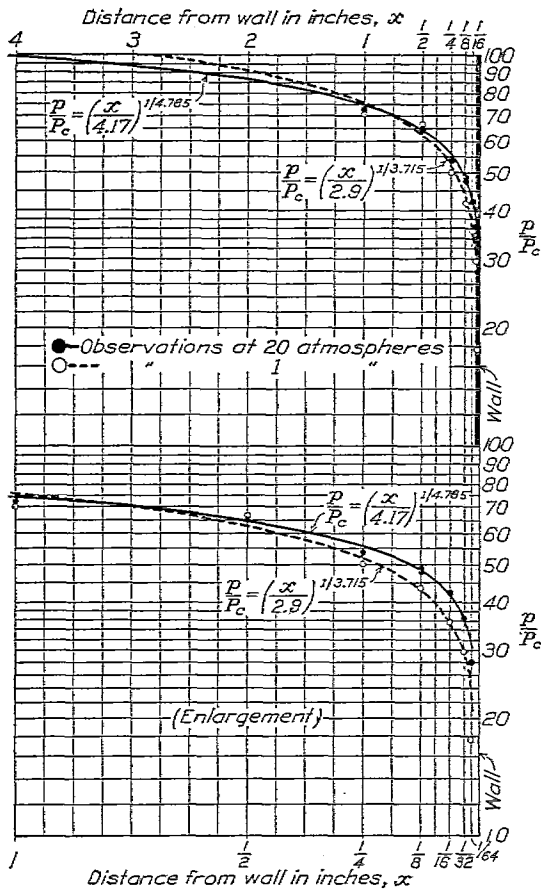


FIG. 29.—Variation of p/P_c with x

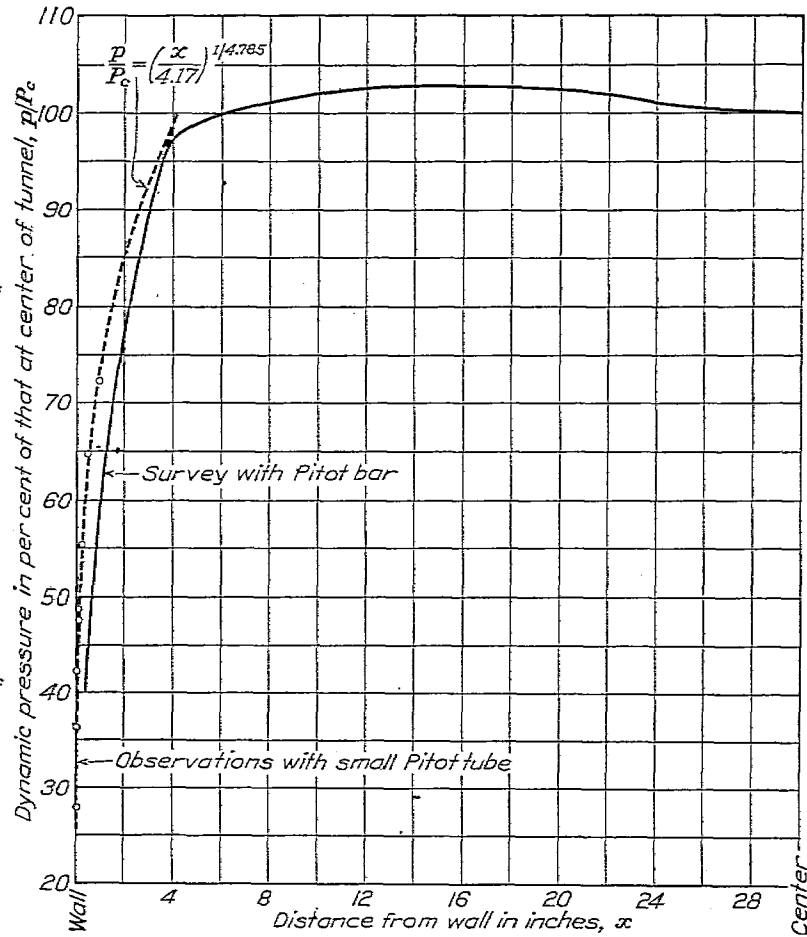


FIG. 30.—Variation of p/P_c with x , 20 atmospheres

Von Karman divides this layer into two regions, one of laminar flow close to the wall and the second of turbulent flow outside of the first. For these conditions he has derived equations for the variation of the velocity near the wall. For the laminar region, he gives:

$$v = \frac{\tau_o}{\mu} x,$$

where v = velocity at the point parallel to the wall.

τ_o = shearing stress at the surface $\mu \left(\frac{\partial v}{\partial x} \right)_{x=0}$

μ = viscosity of the air.

x = distance from the wall or surface.

For the turbulent flow, the following equation is given:

$$v = V_c \left(\frac{x}{\delta} \right)^{1/7}$$

where V_c = velocity at the center of the tunnel.

δ = total thickness of the boundary layer in the direction of x .

The experimental work at Delft of Van der Hegge Zijnen (reference 5) on the boundary layer close to a smooth glass plate, gives an excellent opportunity for comparison with the above theoretical equations. Such a comparison shows very good agreement.

In view of the above, it is interesting to note the agreement that is obtained between the results from Delft and those of this investigation at 1 atmosphere. In Figure 27 there are plotted values of v/V_c for respective values of x with curves drawn for each pressure or density. The velocity in the center of the tunnel for the condition of 1 atmosphere tank pressure is, from Figure 28, 20.2 m/s; on the same plot (fig. 27) there is given the data obtained at Delft for 20 m/s. When plotted on logarithmic scales the straight portion of the curve corresponds to the turbulent region wherein the relation $v/V_c = \left(\frac{x}{\delta} \right)^n$ holds and the curved portion, to the laminar region (reference 5). In each case the laminar flow region extends to about the same distance from the wall, point A. In the remaining portion the two curves are about parallel, though displaced from one another. The large boundary layer shown by the results of this research is no doubt due to the comparative roughness of the tunnel wall and to the continuous (longitudinal) surface of the wall.

The effect of the change in density may be seen in Figures 27, 28, and 29. The depth of the boundary layer, which was found by extrapolation, increases as the density becomes greater. The reciprocal of the exponent n of the equation $\frac{v}{V_c} = \left(\frac{x}{\delta} \right)^n$ has been plotted in Figure 28, where its variation with density may be seen. At 20 atmospheres a value of n of $\frac{1}{9.57}$ was obtained, a considerable change from the 1 atmosphere value of $\frac{1}{7.43}$. The latter figure is in the neighborhood of the values obtained by other experimenters at a density of 1 atmosphere. One might conclude from an inspection of the above figures that as the density is increased the mass of inertia effect becomes more prominent in comparison to the viscosity effect; at the high densities the velocity gradient in the turbulent portion of the boundary layer is less and in the laminar portion greater.

CONCLUSION

This investigation has shown good agreement with previous researches, and has shown that there is a "scale effect" as the density of the fluid is increased; the "scale effect" found is, primarily, a decrease in the exponent n of the Von Karman formula,

$$\frac{v}{V_c} = \left(\frac{x}{\delta} \right)^n$$

which defines the flow of a fluid in the boundary layer at the surface (in this case, of the wind tunnel).

REFERENCES

1. MUNK, MAX M., and MILLER, ELTON W. The Variable Density Wind Tunnel of the National Advisory Committee for Aeronautics. N. A. C. A. Technical Report No. 227, 1925.
2. PRANDTL, L. Applications of Modern Hydrodynamics to Aeronautics. Part II, section F. N. A. C. A. Technical Report No. 116, 1921.
3. GLAUERT, H. The Interference of Wind Channel Walls on the Aerodynamic Characteristics of Airfoil. Reports and Memoranda No. 867, March, 1923. British Aeronautical Research Committee.
4. VON KARMAN, TH. "Zeitschrift für angewandte Mathematik und Mechanik" I, 1921.
5. ZIJNEN, B. G., Van der Hegge. Measurements of the Velocity Distribution in the Boundary Layer Along a Plane Surface. Mededeeling No. 6. "Uit het Laboratorium voor Aerodynamica en Hydrodynamica der Technische Hoogeschool te Delft," 1924.

TABLE I
VELOCITIES CLOSE TO WALL OF TUNNEL IN PLANE OF MODEL

[0.051 inch hypodermic tube used as pitot]

Pressure atm.	Density ρ	Pitot at center		Pitot at wall		Distance from wall		v/V_0 %
		P_c kg/m ²	V_c m/s	P_w kg/m ²	v m/s	x in.	x cm	
1.012	0.1234	25.45	20.31	18.1	17.10	1.00	2.54	84.2
2.495	.3095	67.3	20.85	49.5	17.88	1.00	2.54	85.8
5.10	.6270	139.5	21.09	102.0	18.04	1.00	2.54	85.6
10.27	1.235	290.0	21.68	212.2	18.55	1.00	2.54	85.6
9.92	1.202	278.0	21.50	204.0	18.43	1.00	2.54	85.7
20.36	2.480	613.0	22.34	442.0	18.88	1.00	2.54	84.5
10.34	1.261	287.0	21.35	205.2	18.04	1.00	2.54	84.5
5.24	.6470	142.8	21.00	104.8	17.99	1.00	2.54	85.7
2.57	.3145	66.6	20.58	49.5	17.74	1.00	2.54	86.2
1.01	.1228	25.0	20.19	17.4	16.84	1.00	2.54	83.4
1.026	.1281	26.5	20.34	17.52	16.54	1/2	1.27	81.3
10.20	1.240	286.0	21.48	187.4	17.40	1/2	1.27	81.0
20.20	2.390	594.0	22.30	384.0	17.92	1/2	1.27	80.4
1.025	.1265	25.5	20.07	12.78	14.21	1/4	.635	70.8
10.20	1.222	282.0	21.49	153.2	15.85	1/4	.635	73.8
20.75	2.475	598.0	22.00	320.7	16.10	1/4	.635	73.2
1.008	.1247	25.1	20.05	13.35	14.63	1/4	.635	72.9
1.020	.1280	25.6	20.01	11.2	13.23	1/8	.318	66.6
2.515	.3105	66.1	20.65	30.8	14.08	1/8	.318	68.2
4.90	.6000	133.1	21.07	63.6	14.57	1/8	.318	69.2
10.20	1.230	280.2	21.35	137.2	14.95	1/8	.318	70.0
9.04	1.132	262.2	21.52	126.6	14.96	1/8	.318	69.4
20.55	2.478	612.0	22.26	298.5	15.53	1/8	.318	69.8
20.55	2.478	611.0	22.22	295.0	15.43	1/8	.318	69.4
5.24	.6300	142.0	21.22	68.0	14.69	1/8	.318	69.2
2.31	.2870	60.8	20.58	27.8	13.93	1/8	.318	67.7
1.020	.1258	25.76	20.22	10.5	12.93	1/8	.318	63.9
1.021	.1249	25.5	20.21	9.14	12.10	1/16	.159	59.9
1.021	.1249	25.5	20.21	9.06	12.04	1/16	.159	59.6
2.525	.3070	65.6	20.67	25.74	12.96	1/16	.159	62.7
2.525	.3070	65.8	20.70	25.74	12.96	1/16	.159	62.6
5.10	.6130	137.6	21.17	55.8	13.50	1/16	.159	63.8
10.35	1.229	286.2	21.60	119.4	13.94	1/16	.159	64.5
20.30	2.380	580.0	22.07	239.9	14.21	1/16	.159	64.4
20.20	2.375	582.0	22.14	246.1	14.39	1/16	.159	65.0
20.40	2.400	581.0	22.00	246.9	14.34	1/16	.159	65.2

TABLE II
 VELOCITIES CLOSE TO WALL OF TUNNEL IN PLANE OF MODEL
 [0.019 inch Dural tube used as pitot]

Pressure atm.	Density ρ	Pitot at center		Pitot at wall		Distance from wall		v/V_c %
		P_c kg/m ²	V_c m/s	p kg/m ²	v m/s	x in.	x cm	
1. 015	. 1253	25. 6	20. 21	11. 23	13. 39	1/8	. 318	66. 2
10. 20	1. 222	284. 5	21. 58	135. 6	14. 90	1/8	. 318	69. 1
10. 20	1. 222	284. 5	21. 58	132. 8	14. 74	1/8	. 318	68. 3
20. 47	2. 405	596. 0	22. 27	277. 0	15. 17	1/8	. 318	68. 4
20. 47	2. 393	588. 0	22. 18	279. 5	15. 27	1/8	. 318	68. 3
1. 017	. 1250	25. 6	20. 33	9. 0	12. 00	1/16	. 159	59. 3
2. 535	. 3070	65. 5	20. 66	25. 1	12. 78	1/16	. 159	61. 9
5. 10	. 6090	135. 8	21. 11	55. 3	13. 48	1/16	. 159	63. 9
10. 27	1. 242	290. 0	21. 60	123. 3	14. 10	1/16	. 159	65. 3
20. 60	2. 420	604. 0	22. 34	259. 5	14. 64	1/16	. 159	65. 5
1. 015	. 1238	25. 5	20. 30	7. 6	11. 08	1/32	. 0795	54. 6
10. 20	1. 211	281. 0	21. 54	99. 0	12. 79	1/32	. 0795	59. 4
20. 50	2. 395	586. 0	22. 20	211. 0	13. 27	1/32	. 0795	59. 8
1. 020	. 1231	25. 1	20. 01	4. 4	8. 45	1/64	. 040	41. 8
10. 20	1. 198	274. 0	21. 60	72. 4	11. 00	1/64	. 040	50. 9
20. 25	2. 360	580. 0	22. 16	162. 2	11. 72	1/64	. 040	52. 9